Carbon Materials as Positive Electrodes in Bromine-Based Flow Batteries
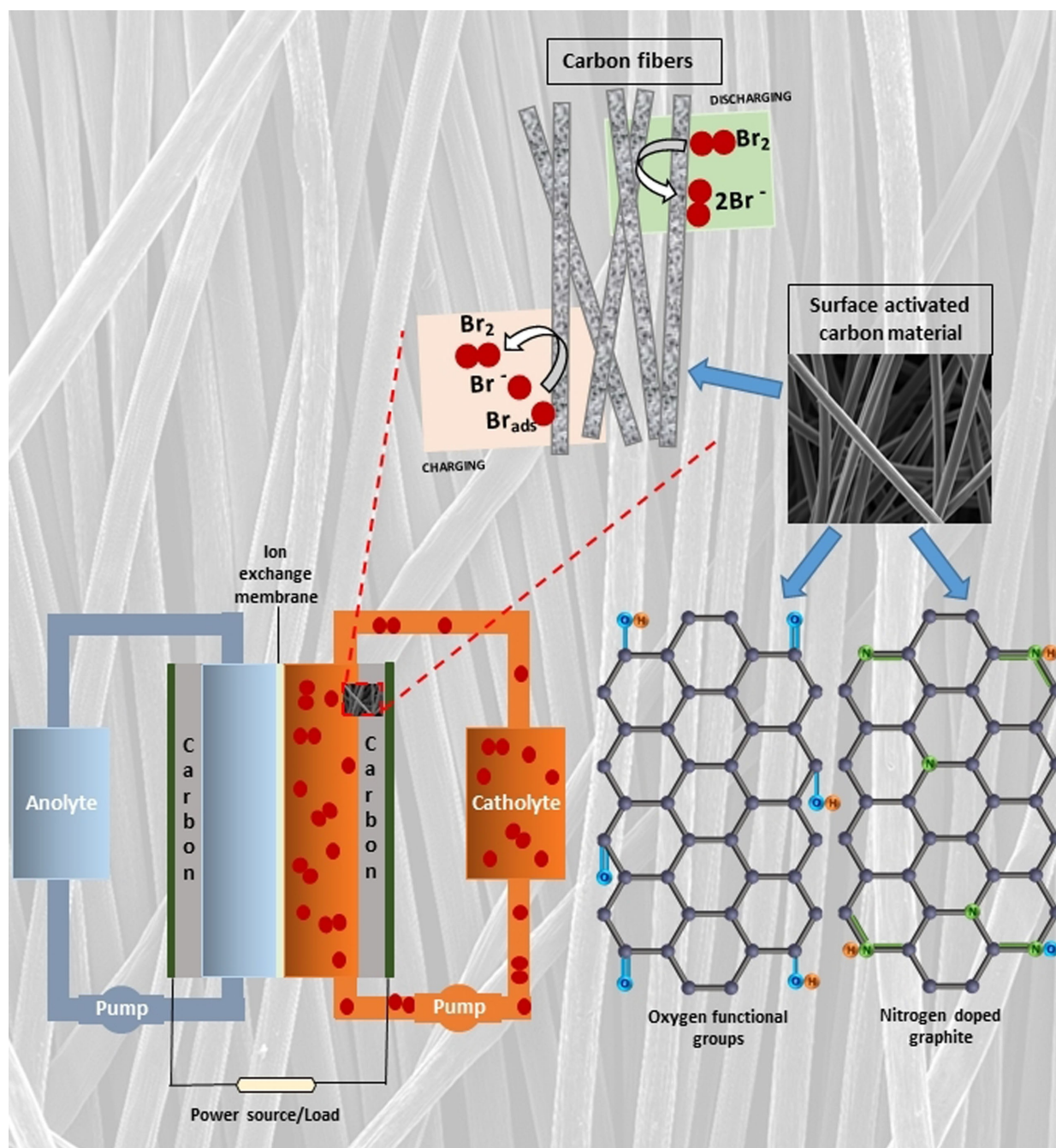
Yaksh Popat,[a] David Trudgeon,[a] Caiping Zhang,[b] Frank C. Walsh,[c] Peter Connor,[a] and Xiaohong Li*[a]

Bromine based redox flow batteries (RFBs) can provide sustainable energy storage due to the abundance of bromine. Such devices pair Br_2/Br^- at the positive electrode with complementary redox couples at the negative electrode. Due to the highly corrosive nature of bromine, electrode materials need to be corrosion resistant and durable. The positive electrode requires good electrochemical activity and reversibility for the Br_2/Br^- couple. Carbon materials enjoy the advantages of low cost, excellent electrical conductivity, chemical resistance, wide operational potential ranges, modifiable surface properties, and high surface area. Here carbon based materials for bromine electrodes are reviewed, with a focus on application in zinc-bromine, hydrogen-bromine, and polysulphide-bromine RFB systems, aiming to provide an overview of carbon materials to be used for design and development of bromine electrodes with improved performance. Aspects deserving further R&D are highlighted.

1. Introduction

Renewable energy sources are expected to play a vital role in the transition to a highly energy-efficient and low carbon economy, but its natural fluctuation character represents a major barrier to the maximum consumption of renewables. To this, energy storage systems (ESS) can act as a buffer between power generation and consumers, making a real difference in managing demand and supply to create a more resilient energy infrastructure and bring cost savings to consumers.[1,2] Redox flow batteries (RFBs) represent one class of electrochemical energy storage technologies[3–7] and have a number of advantages over other type of ESS, including flexibility, deep-discharge capability, rapid response, and safe operation. RFBs are therefore one potential solution to large scale energy storage essential to the integration of widespread renewable energy into a national energy supply system.[8–11] As shown in Figure 1, RFBs convert electrical energy to chemical energy during charge and release the electricity back during discharge. Unlike traditional batteries that store energy in active electrode materials, RFBs store energy within the electrolyte and are sometimes referred to as regenerative fuel cells.

The key feature of RFB is the separation between power and energy capacity of the system, where the energy capacity of a RFB is determined by the volume of the electrolyte and the concentration of the electroactive species, while the power depends on the size of the electrode and the number of cells in the stack. This means that the power and energy capacity of RFBs can be easily varied, hence the flexibility of the energy storage is enhanced. If more energy is needed in a RFB system, only the capacity of the electrolyte needs to be increased. If more power is needed, only additional cells need to be added. This is a great advantage over other traditional battery storage systems.[12–14]

In general, RFBs are seen as a promising energy storage technology for grid-scale applications but they have to demonstrate themselves as competitive technologies to reach the performance required at the level of practical application. For example, more recently some aqueous RFB systems with organic redox couples have been studied extensively owing to their low cost and good cycling performance.[15–19] To maximise competitiveness, the electrolyte and the electrode materials in RFB systems need to be low cost; selecting for an abundant material offers obvious advantages in realising economical energy storage. Among the RFB family, the bromine-based redox flow battery is such a promising candidate, with a high potential to make a breakthrough at this point.

Bromine-based RFBs meet the electrolyte requirements owing to the abundance, e.g. 380,000 metric tons worldwide production of bromine in 2018.[20–23] Bromine-based flow batteries, consisting of Br_2/Br^- and another redox couple, show the advantages of high theoretical energy density and low cost.[1,20] Due to the highly corrosive nature of bromine, electrode materials for bromine need to be corrosion resistant, durable and cheap as well as demonstrating good electrochemical activity. Noble metal platinum shows excellent electrochemical activity for bromine redox reactions but its instability in bromine electrolytes and high cost hampers its use.[21–23] Carbon materials possess the advantages of moderate cost, excellent electrical conductivity, inertness to corrosive media, a wide operational potential range, controllable surface properties, high surface area, suitable porosity and simple synthetic methods.[1,2,20,24,25]

There are several reviews[4–7] which critically discuss technical, economic and environmental aspects of redox flow battery. Readers who may be interested in RFBs' proposed chemistries, progress and challenges, cell components and design considerations, as well as for cost comparison between chemical elements,[26] are referred to those reviews. This review is focussed on carbon-based electrode materials in three bromine based RFBs namely, zinc-bromine battery (ZBB), hydrogen-bromine battery (HBB) and polysulphide-bromine battery (PSBB). In particular, rather than examine the electrode material

[a] Y. Popat, D. Trudgeon, P. Connor, X. Li
Renewable Energy group
College of Engineering
Mathematics and Physical Sciences
University of Exeter
Penryn campus, Cornwall, TR10 9FE (United Kingdom)
E-mail: x.li@exeter.ac.uk
[b] C. Zhang
National Active Distribution Network Technology Research Centre
Beijing Jiaotong University
Beijing 100044 (P. R. China)
[c] F. C. Walsh
Electrochemical Engineering Laboratory
Energy Technology Research Group
Engineering Sciences and the Environment
University of Southampton
Southampton SO17 1BJ (United Kingdom)

ChemPlusChem

Review
doi.org/10.1002/cplu.202100441

Chemistry Europe
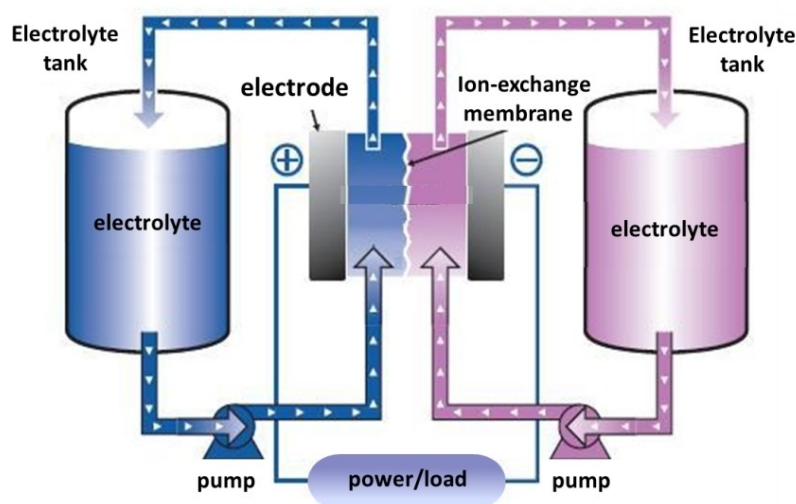European Chemical
Societies Publishing

Figure 1. Principle of redox flow battery (RFB). Reproduced from ref. [5] with permission from RSC publication.

Yaksh Popat received his B.Sc and M.Sc in physics from University of Mumbai (India). Thereafter, he completed his PhD in physics from University of Trento (Italy), developing nanocatalyst coatings for applications in water purification and hydrogen production. In 2020, Yaksh joined the University of Exeter (UK) as a postdoctoral research fellow on the Horizon 2020 project "MELODY" working on hydrogen bromine redox flow battery. His research interests include nanostructured materials (powders/thin films) for photocatalysis and electrocatalysis, electrolysers for clean hydrogen production and redox flow batteries for energy storage.

David Trudgeon gained a BSc in Renewable Energy from the University of Exeter in 2015, where he was awarded his PhD in Energy Storage in 2020. He is now a research fellow within the Renewable Energy Group at the University of Exeter. David's research experience includes electrode materials, electrolyte composition and cell design for electrochemical energy storage devices. He has particular experience in membrane free redox flow batteries.

Caiping Zhang received her BSc degree in vehicular engineering from the Henan University of Science and Technology in China in 2004 and PhD degree in vehicle engineering from the Beijing Institute of Technology in China in 2010. She is currently a Professor in Beijing Jiaotong University. Her research interests focus on battery modeling, health diagnosis and prognosis, battery smart management, and fault diagnosis of lithium ion batteries used in electric vehicles and energy storage system.

Professor Frank C Walsh is Emeritus Professor of Electrochemical Engineering within Engineering and Physical Sciences at the University of Southampton. Frank Walsh holds the degrees of BSC (Applied Chemistry), MSc (Materials Protection) and PhD (Electrochemical Engineering) following periods of study at from the Universities of Portsmouth, UMIST and Loughborough. Frank has expertise in electrochemical engineering (fuel cells and environmental treatment), corrosion engineering and synthesis of materials, electroplating and plasma anodizing as engineering coatings, and nanostructured materials via electrochemistry.

Peter Connor completed his BSc Chemistry at the University of Warwick in 1992. He went on to complete an MSc in Environmental Monitoring and Assessment at Coventry University in 1996 and then a PhD in Renewable Energy at the UK's Open University in 2002. Postdoctoral work took him back to Warwick before he accepted a lectureship at the University of Exeter's new Penryn campus in 2005, joining Exeter's emergent Renewable Energy department where he is now an Associate Professor.

Xiaohong Li is a professor of energy storage and director of global development in Renewable Energy Group at the University of Exeter. She holds a PhD in Physical Chemistry from joint education of Peking University and Lanzhou University, a MSc in Analytical Chemistry and a BSc in Organic Chemistry from Lanzhou University. Her research interest is focused on energy storage with an emphasis on redox flow batteries, anion exchange membrane water electrolysers for hydrogen production, and nanoscale materials for electrocatalysis.

ChemPlusChem

Review
doi.org/10.1002/cplu.202100441

**Chemistry
Europe**

European Chemical
Societies Publishing

used in each of full systems, this paper aims to evaluate key parameters of potential carbon materials for the design of bromine electrodes with higher electrochemical activity and stability and to provide a comprehensive summary of these materials as the side of bromine electrodes in the three RFB systems.

2. Mechanism of Bromine/Bromide Redox Reactions

2.1. Three Proposed Mechanisms

The mechanism of bromine oxidation and reduction reactions at a platinum electrode were studied during the 1960s and 1980s and onwards.[27–37] In general, three mechanisms have been proposed for bromine electrode reaction: (i) the Volmer-Heyrovsky (V-H), (ii) the Volmer-Tafel (V-T) and, (iii) the Heyrovsky-Tafel (H-T). The kinetics of the Br_2/Br^- reaction was found to be fast on both reduced and oxidized Pt electrodes. The bromine electrode reaction can be expressed by (1):

$$2\,Br^- - 2\,e^- \rightleftharpoons Br_2 \tag{1}$$

On the anodic process, molecular bromine is formed by oxidation of Br^- ions with a reverse reaction occurred on the cathodic process. The reaction can be divided into several steps. As in the case of the anodic process, the first step is a Volmer reaction, where adsorbed bromine atoms are formed by discharge of Br^- ions.

$$Br^- \rightleftharpoons Br_{ad} + e^- \;(\text{Volmer reaction}) \tag{2}$$
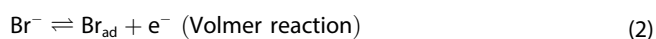
Molecular bromine can then be formed according to either of the two following steps. Discharge of Br^- ions on adsorbed bromine atoms

$$Br^- + Br_{ad} \rightleftharpoons Br_2 + e^- \;(\text{Heyrovsky reaction}) \tag{3}$$

or combination of adsorbed bromine atoms

$$2\,Br_{ad} \rightleftharpoons Br_2 \;(\text{Tafel reaction}) \tag{4}$$

Overall, based on the qualitative comparison of the predictions of the models, it has been shown that either the Volmer-Heyrovsky mechanism or the Volmer-Tafel mechanism with the Volmer reaction controlling is a well-acceptable mechanism for the Br_2/Br^- reaction, which can be used to predict current density-overpotential curves.[30,31]

At a stationary graphite electrode, the mechanism of electrochemical bromine evolution was elucidated by Jassen and Hoogland.[32] They suggested that bromine was formed according to the Volmer-Heyrovsky mechanism but argued the Heyrovsky reaction was the rate determining step (rds). Mastragostino and Gramellini[33] studied the Br_2/Br^- redox reaction at two different vitreous carbon electrodes, reticulated
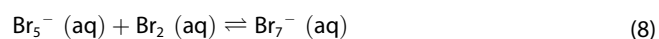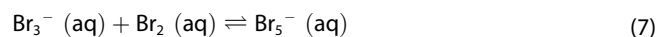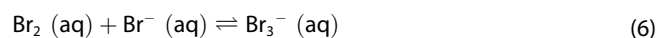
vitreous carbon and smooth vitreous carbon, and they carried out the study using the rotating disc electrode method to compare a series of rate constants of the Br_2/Br^- reactions at the two electrodes. They found that the different materials did not affect the reaction mechanism. On both electrodes the cathodic and the anodic processes involves two consecutive electrochemical steps: Volmer reaction and Heyrovsky reaction. The Volmer reaction of the adsorption of Br^- anion at the electrode surface is the rds in the cathodic process while the Heyrovsky reaction of the combination of Br^- anion and Br atom is the rds in the anodic process. The Br_3^- reduction occurs via formation of Br_2, with which Br_3^- is in rapid equilibrium, whereupon Br_2 is reduced according to V-H mechanisms.

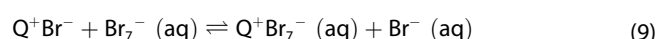### 2.2. Mechanism and Kinetics with BSAs at Electrode

Very little free bromine exists in the bromine-based flow battery. Bromine is present as polybromide ions dissolved in the aqueous portion of the electrolyte, which is described as follows:

$$nBr_2 + Br^- = Br_{2n+1}^- \;(n = 1,\,2,\,3) \tag{5}$$
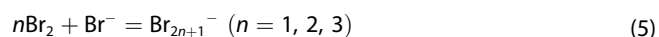
In solution, elemental bromine exists in equilibrium with bromide ions to form polybromide ions, that is, tribromide ions (Br_3^-) are formed first, then pentabromide (Br_5^-) and eventually heptabromide (Br_7^-).[34–40] The reactions are:

$$Br_2\,(aq) + Br^-\,(aq) \rightleftharpoons Br_3^-\,(aq) \tag{6}$$

$$Br_3^-\,(aq) + Br_2\,(aq) \rightleftharpoons Br_5^-\,(aq) \tag{7}$$

$$Br_5^-\,(aq) + Br_2\,(aq) \rightleftharpoons Br_7^-\,(aq) \tag{8}$$

The Br_3^- formation (reaction 6) occurs at the near electrode surface, while Br_5^- (reaction 7) and Br_7^- (reaction 8) formations occur in the solution. The bromine-based RFBs exhibit rapid self-discharge and poor faradaic efficiency. Take the ZBB system as an example, the high solubility of bromine in the electrolyte leads to a consequent high rate of transport to the zinc deposit. One method of overcoming this problem is using an ion-exchange membrane between the two electrodes. However, ion-exchange membranes are usually expensive but also have a low rate of bromine transport. In order to use much less costly porous polyethylene or polypropylene separators, the effective bromine concentration in the positive-side electrolyte needs to be reduced. This can be done by using suitable bromine sequestration agents (BSAs) which are usually quaternary ammonium bromide (QBr, where Q is quaternary ammonium cation) salts. For example,

$$Q^+Br^- + Br_7^-\,(aq) \rightleftharpoons Q^+Br_7^-\,(aq) + Br^-\,(aq) \tag{9}$$

$$Q^+Br_3^- + Br_2 \rightleftharpoons Q^+Br_5^- \tag{10}$$

$$Q^+Br_5^- + Br_2 \rightleftharpoons Q^+Br_7^- \tag{11}$$

A variety of BSAs can be used to capture and store these bromine species evolved at the positive electrode during charge. However, Cathro et al.[36,37] examined four cyclic- and eleven alkyl-quaternary ammonium bromides and found that no single compound proved entirely acceptable. If only utilising one of these BSAs, solid phase formations are inevitably formed which prevent electrolyte circulation and could eventually lead to cell failure. Cedzynska[38] carried out quantitative tests for the mixture of cyclic, unsymmetrical and symmetrical aliphatic QBr compounds, and identified a modified QBr mixture containing four QBr compounds: N-methyl-N-ethyl morpholinium (MEM) bromide, N-methyl-N-ethyl pyrrolidinium (MEP) bromide, diethyl-methyl propylammonium bromide, and tetrabuthylammonium bromide with the molar ratio of 0.50:0.25:0.15:0.10. The modified electrolyte allowed the zinc-bromine cell to be operated within the temperature range of 278–323 K and outperformed the conventional electrolyte containing a single QBr or two QBr compounds.

Further studies by Bauer et al.[39] in 1997 and Kautek et al.[40] in 2001 showed that MEM exhibits a much stronger chemical affinity to carbon surface than MEP, which result in a slow conversion process for the adsorbed MEM-Br ion pairs. The authors reported that in the electrolyte a higher concentration of MEP than that of MEM is favourable to increase the zinc-bromine cell efficiency. For example, Kautek et al suggests a concentration ratio of 3:1 between MEP and MEM.

3. Carbon Based Materials for the Bromine Electrode

Numerous carbon based materials have been reported in literature for a variety of industrial applications owing to their low cost, tunable structural properties, abundance, ease of fabrication, stability and good electronic properties. Carbon/graphite felt, carbon paper, reticulated vitreous carbon (RVC), carbon cloth, activated carbon, carbon polymer and carbon nanotubes (CNTs) are amongst the widely demonstrated electrode materials for experiments.[41–50] Though different carbon materials have a lot of common features adherent to the fundamental properties of carbon, based on their fabrication process, they still differ from each other, exhibiting peculiar features and morphologies.

Carbon and graphite felts are widely used 3D materials made from two kinds of precursors namely, polyacrylonitrile (PAN) and rayon (regenerated cellulose), via a needle punching process followed by graphitization. The internal structure, textile structure, thickness, homogeneity of the felts is dictated by needle punching and hence is a crucial step. The felt materials are then thermally treated at 1200–1600°C to obtain carbon felts. Further graphitization of carbon felts to 2000–2600°C forms graphite felts as shown in Figure 2b. Different parameters during the process stage can lead to different electrical as well as physical properties of the produced felts.[41–43]
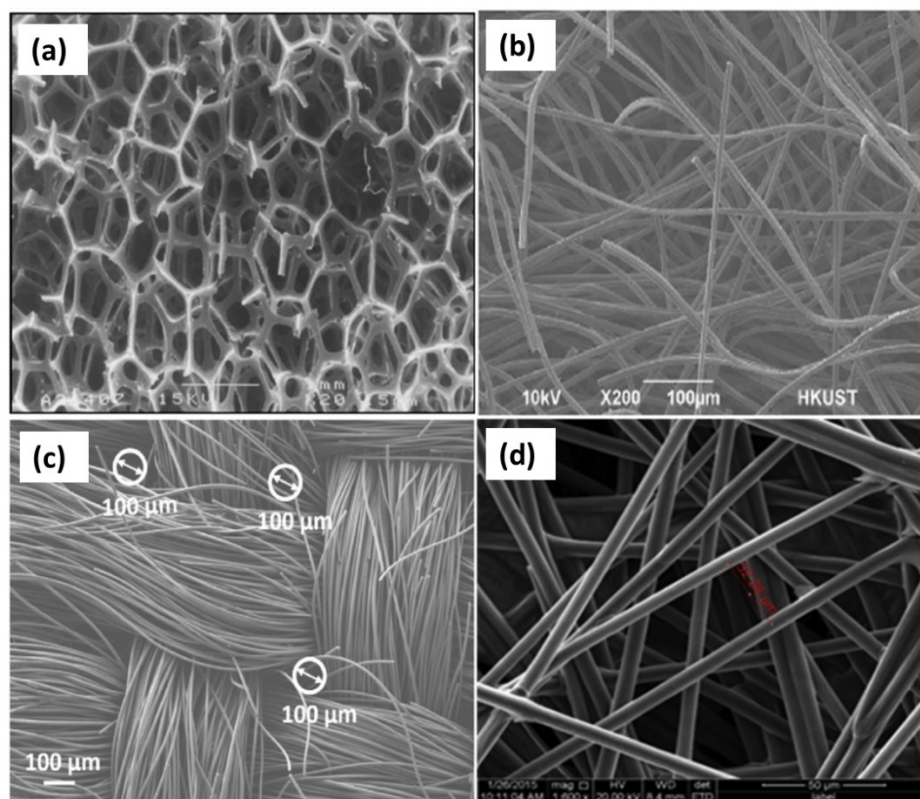

Figure 2. SEM images of [a] RVC[46] [b] graphite felt[49] [c] carbon cloth[45] and [d] carbon paper.[44] Reproduced from refs. [44–46,49] with permission from Elsevier.

Carbon paper on the other hand, consists of a cluster of crisscrossing carbon fibers having pores in the interlaced carbon fibers[44] (Figure 2d). In general, the carbon paper is much thinner (100–400 μm) than the felts (2.5 mm–10 mm) thereby demonstrating a clear distinctive feature for applications where minimum thickness is desired. Carbon paper has been widely used as a gas diffusion layer for high performance fuel cells due to its good electrical and thermal conductivities, lightweight, chemical stability, corrosion resistance and high porosity (above 70% for gases and liquids). Commercial carbon paper is hydrophobic and generally has low specific surface area, therefore prior to being utilized as electrodes, it requires appropriate surface treatments to improve the properties of hydrophilicity, conductivity, and electroactive activity.

Carbon cloth is a highly conductive textile with a three dimensional network which is made by weaving the carbon fiber and has a relatively more ordered fiber arrangement pattern and a broad pore distribution from 5 to 100 μm as shown in Figure 2c. The lower tortuosity and higher permeability as compared with carbon paper under the same fiber diameter and porosity may result in excellent transport properties.[45] Further, as described, carbon paper is non-woven while carbon cloth is woven fabric, thus no binder is normally needed for carbon cloth.

Vitreous carbon displays low density, reduced thermal expansion, good corrosion resistance and excellent thermal and electrical conductivities. The RVC (an open foam material), composed solely of vitreous carbon, has a honeycomb structure enhancing the catalytic sites (see Figure 2a). This structure is achieved by polymerization of a resin combined with foaming agents and subsequent carbonization. Firstly, the foam resin is dried and cured at 120°C, followed by carbonization at 700–1100°C.[46]

Physical (thermal) and/or chemical activation of carbonaceous materials (e.g. wood, coal, nutshell) are carried out to synthesize activated carbons (ACs). Physical activation usually refers to the thermal treatment of carbon precursors in the temperature range of 700 to 1200°C in presence of oxidizing gases like steam, CO_2 and air. Chemical activation is generally carried out at lower temperatures (400 to 700°C) with activating agents such as H_3PO_4, KOH, NaOH and $ZnCl_2$. The activation

methods and the carbon precursors play an important role in the physicochemical properties of the synthesized ACs.[47]

Carbon polymer composites (CPCs) have a strong physical advantage over other commercial carbon materials due to the enhanced mechanical stability provided by the polymer structure. Conducting carbon polymer composites not only exhibit low electrical resistance but also light weight, low cost and flexibility. Injection moulding, a low-cost method for producing large quantities of carbon materials, can be used for binding together carbon-polymer composite materials with the help of polymer binders like polyvinylidene fluoride (PVDF), high density polyethylene (HDPE), polyvinyl alcohol (PVA), and polyolefin. Performing compression moulding on the expanded graphite with thermoplastic polymers would lead to the manufacturing of a polymer-impregnated graphite plate. Since the compression moulding technique allows the use of a higher ratio of graphite than the injection moulding process, it has superior electrical conductivity. The thermoplastic properties of the polymer employed in this method lead to better thermo-mechanical properties, chemical resistance and thermal stability compared to the composites produced by injection moulding.[48]

Successful materials must have a high activity for the bromine reaction and large specific surface areas, while maintaining high conductivity to minimise ohmic losses and reduce the area specific resistance (ASR) of the cell. Based on the design of the flow battery, certain parameters like material porosity, pore-size distribution, and thickness play a dominating role and dictate the performance of the battery. It is therefore crucial to have appropriate parameters for the carbon material to deliver optimum performance under the required conditions. Some of the commercially available carbon materials for bromine based batteries reported in literature have been listed in Table 1.

In addition, different modification techniques have been used for these carbon electrodes to further enhance their performance by introducing surface functional groups and improving their surface area by acid treatment, thermal treatment, chemical treatment, CO_2 activation and plasma surface treatment with NH_3. For example, the presence of carboxyl and hydroxyl groups, which particularly increases the hydrophilicity and catalytic activity towards the bromine reaction, is most

Table 1. List of commercially available carbon materials reported for bromine based RFBs.

Carbon materials	Model	Type	Thickness [mm]	Porosity [%]	Electrical resistivity [Ω-mm]	Surface area [m²g⁻¹]	Reference
Carbon felt	KFD 2.5 EA	PAN	2.50	90	<10	0.6	[51]
	–	PAN	3.20	90	4	–	[52]
	–	PAN	5.00	92	22.2	0.12	[53]
Graphite felt	GFA5	Graphite soft felt	6.00	90	0.7	–	[54,55]
	GFD 4.65 EA	PAN	4.60	94	<3	0.4	[51,56]
	JL ZMC	PAN	5.00	90	–	1.1	[57]
Carbon paper	PCP	Carbon fiber paper	0.28	70	10	–	[58,59]
	SGL 10AA	Carbon fiber paper	0.22	82	<5	1.0	[60,61]
	SGL 29AA	Carbon fiber paper	0.19	88	<5	0.2	[61,62]
	2050A	Carbon fiber paper	0.38–0.40	78	0.15	–	[63,64]
Carbon cloth	ELAT hydrophilic Plain	Carbon fiber cloth	0.40	80	1.1	2.39	[45,65]

ChemPlusChem

Review
doi.org/10.1002/cplu.202100441

Chemistry
Europe
European Chemical
Societies Publishing

commonly achieved by pre-treatment in sulphuric acid or sulphuric/nitric acid mixtures at temperatures of 50 °C to 80 °C for 5 to 10 hours.[66–70] Similarly, annealing (thermal treatment) of carbon materials in oxygen/nitrogen environments not only enhances the hydrophilicity but also increases the surface area of the material.[66,71,72]

Park *et al.* observed an increase in the carrier mobility and concentration accompanied by a decrease in the resistivity of the prepared carbon thin films, upon thermal treatment.[73] This behaviour was attributed to the increase of sp^2 bonding fraction and ordering sp^2 clusters caused by increasing annealing temperature in the carbon networks. Prolonged oxidation time at lower temperatures result in low material loss rate, whereas shorter oxidation time at higher temperatures cause elevated material loss. Excessive thermal treatment of positive electrode can show detrimental effect whereas there is consensus that oxidative pre-treatment of the negative electrode enhances its electrochemical activity.[74–76] Upon thermal treatment, the considerable variations observed in the electrical double layer capacitance and loss of mass of two different felts of the same type are worth consideration.[77]

4. Carbon-Based Bromine Electrodes in RFB Systems

4.1. In Zinc-Bromine Redox Flow Battery

Among the RFBs technology family, the zinc-bromine battery (ZBB) has been one of the most developed and commercially scaled-up flow battery systems, designed and developed for load levelling applications from the mid-1970s to date, with a massive research effort made to scale-up and demonstrate ZBBs between the mid-1970s and 1980s.[5,6] For example, 3, 10 and 20 kWh submodules were deployed in 1983 and a 1MW/4MWh zinc-bromine RFB system was installed in Japan in 1990.[3] At present, ZBBs are developed and manufactured by five companies around the world: ZBB Energy Corporation and Premium Power in USA, RedFlow Ltd in Australia, ZBEST Power and Smart Energy in China. These companies produce the battery modules that are expandable from 50 kWh to 500 kWh and available for commercial applications.

In comparison with other RFBs, ZBB possesses two particular advantages that make them outstanding in their applications: (1) high specific energy (70–80 Wh kg^{-1}) and high cell voltage (1.85 V), which lead to enhanced power density and thus devices with a lighter weight; (2) cost-competitiveness: both zinc and bromine are low cost and abundant. Operation of the battery is based on the following reactions as shown in Figure 3.

Negative electrode:

$$Zn^{2+} + 2e^- \rightleftharpoons Zn \tag{12}$$

Positive electrode:

$$2Br^- - 2e^- \rightleftharpoons Br_2 \tag{13}$$

During charge (forward arrows in Equations 12 and 13), metallic zinc is deposited as a thick film on the negative electrode while bromide ions are oxidized to bromine at the positive electrode. During discharge (backwards arrows in Equations 12 and 13), the deposited zinc is oxidised and dissolved into electrolyte; meanwhile, bromine is reduced to bromide ions. Bromine generated at the positive electrode during charge can diffuse from the positive electrode into the zinc negative electrode compartment where it chemically reacts with zinc resulting in a high rate of self-discharge and consequently causing reduction of coulombic efficiency. To avoid this process, a microporous separator or an ion-exchange membrane is required to separate the positive and negative half-cells. In addition to a separator, it is essential to use effective BSAs to capture and store bromine.
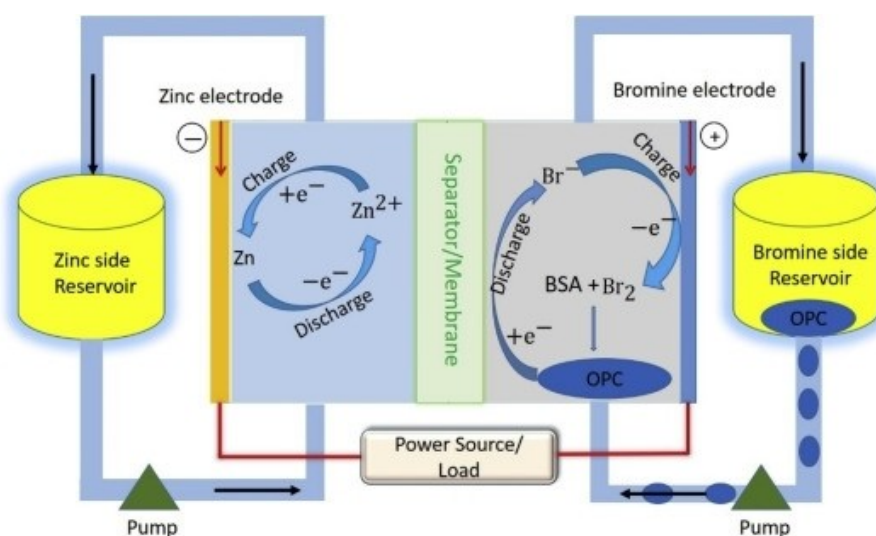

Figure 3. Schematic of a zinc bromine redox flow battery. Reproduced from ref. [78] with permission from Elsevier.

ChemPlusChem

Review
doi.org/10.1002/cplu.202100441

**Chemistry
Europe**
European Chemical
Societies Publishing

Since the Zn/Zn^{2+} couple reacts faster than the Br_2/Br^- couple, this causes polarisation and could eventually lead to battery failure. A higher surface area carbon electrode with higher conductivity is therefore required on the positive electrode side to obtain faster electrochemical reactions and lower polarization.[7] Various carbon-based electrodes material have been extensively studied, some of which are presented as follows.

Carbon and graphite felts have been commonly used as electrode materials in ZBB due to their low cost, good stability, large surface area and high porosity. Lai et al. reported the use of a carbon felt based semi-solid positive electrode in a novel single tank flow cell design.[79] The carbon felt substrate was coated with a mixed active material slurry made by dispersing active carbon powder in $ZnBr_2$ solution. The carbon felt was then marinated in the prepared 6.0 M $ZnBr_2$ solution for 30 s to obtain the semi solid positive electrode with a thickness of 3 mm. This single flow cell can reach a columbic efficiency of 92% and energy efficiency of 82% over 70 cycles at a current density of 20 mA cm^{-2}. Another research group (Suresh et al.)[80] used PAN and rayon based carbon felts in different zinc bromine cell configurations to show the superiority of rayon based CF which exhibited lower charge transfer resistance and increased number of electrochemical active sites as compared to PAN based CF. When operated at a current density of 20 mA cm^{-2}, the cell voltage variation between charge and discharge processes was 200 mV and 300 mV at Rayon based CF and PAN based CF respectively. With Rayon based CF, the cell can reach a columbic efficiency of 96.26%, voltaic efficiency of 83% and energy efficiency of 79.4% over 50 cycles.

Polymer based composites can be produced quickly and possess high mechanical strength and chemical resistance to acidic electrolytes due to their thermoplastic properties.[81] The electrodes are usually made of polymeric materials like HDPE with carbon black or multi walled CNTs as the conductive filler.[82,83] In 1987, Cathro et al. reported the synthesis of plastic bonded carbon (PBC) as bromine electrode for zinc bromine cell.[84] The PBC was prepared as a conductive sheet from a mixture thermoplastic binder (e.g. HDPE, polypropylene) and carbon black powder by hot pressing, injection moulding, or extrusion process. Two-layer bromine electrode structures with the surface layer containing high fraction of carbon black achieved satisfactory electrochemical activity. They reported the best activity was obtained for surface layer containing carbon black with low bulk density and high surface area (e.g. Ketjen black or Black Pearls 2000). The authors also observed some degradation of the best performing bromine electrode after a number of charge/discharge cycles and even without being charge/discharge cycled when the electrode was simply immersed in a bromine-containing solution. They suggested that the loss of carbon black from the surface of the electrode is not the main cause of the performance loss observed, but the degradation of the plastic binder is one important factor.

Low dimensional carbon shows some interesting features when applied in a porous electrode. 2D mesoporous carbon can help in exposing more electrocatalytic active sites, extending the catalytic interface and favouring the mass transfer of reactants.[85,86] Jin et al. investigated low dimensional nitrogen-doped ordered mesoporous carbon (NOMC) as an electrocatalyst for Br_2/Br^- redox reactions in ZBB.[87] The synthesized material displayed good electrochemical activity due to the nitrogen doping and low dimension of carbon which facilitated mass transfer and exposure of nitrogen activated carbon sites. Zinc bromine flow battery constructed with two dimensional nitrogen-doped carbon (NOMC-2D) as porous electrode reported superior performance than NOMC-3D with a high energy efficiency of 84.3% at 80 mA cm^{-2}. This is the highest energy efficiency recorded in the literature for a ZBB at this operating current density.

Nitrogen doping has resulted in an improved electrochemical performance of carbon materials for vanadium redox flow batteries.[88–90] Wu et al. synthesized carbonized tubular polypyrrole (CTPPy) by a facile method to evaluate their performance in ZBB system.[49] The synthesized CTTPy exhibited superior activity for Br_2/Br^- redox reactions due to the abundant nitrogen and oxygen containing functional groups. CTTPy anchored on GF as bromine electrode in zinc bromine flow cell displayed a high energy efficiency of 76% at 80 mA cm^{-2}, with no degradation seen after 100 cycles.

Chemical doping with hetero-atoms can modulate the electronic properties of carbon material. Nitrogen doping can help achieve appropriate electron modulation for electrocatalytic process owing to its higher electronegativity.[91–93] Xiang et al. investigated the use of carbon spheres nitrogen doped in ammonia atmosphere in a tube furnace at temperatures between 900°C and 1100°C for 10 minutes. They report that the total amount of nitrogen decreases with increasing temperature, and that the proportion of graphitic nitrogen increases, while the proportion of pyridinic nitrogen decreases. A zinc bromine flow cell employing carbon spheres doped with nitrogen at 1000°C achieved an energy efficiency of 82.5% at 80 mA cm^{-2}, compared to 76.0% with unmodified carbon spheres.[93]

Wu et al. synthesized N-doped graphene nanoplatelets (N-GnP) by a simple pyrolysis method and applied as a catalyst for Br_2/Br^- redox reactions.[92] The N-GnP anchored on GF showed remarkably good electrochemical activity in an in-house laboratory flow cell with an energy efficiency of 78.8% at a relatively high operating current density of 120 mA cm^{-2} with no degradation over 100 cycles. This is the highest reported activity in ZBB systems at such a high operating current density, attributed to the increased adsorption of bromide species and enhanced charge transfer due to N-doping.

Boron-doped graphene (BDG) is a promising electrode material because of the high surface area and good electrochemical activity.[94–96] Venkatesan et al. reported boron-doped reduced graphene oxide (B-rGO) as bromine electrode catalyst in zinc bromine flow battery to alleviate the sluggish Br_2/Br^- kinetics.[97] B-rGO supported on CF substrate showed improved performance due to high electrical conductivity and electrocatalytic behavior of B-rGO but at a relatively low operating current density of 20 mA cm^{-2}.

Much of the recent research is on the introduction of nanostructured materials such as carbon nanotubes into carbon

polymer composite electrodes to increase surface area and hence the rate of electrode reactions. Munaiah et al.[98] in 2014 reported that single-walled carbon nanotube (SWCNT) and multi-walled carbon nanotube (MWCNT) modified carbon felt as positive electrodes exhibits improved electrochemical activity for Br_2/Br^- redox reaction. In 0.05 M $ZnBr_2$ aqueous solution, they reported the electrochemical activity for Br_2/Br^- redox reaction exhibits in the order of SWCNT > MWCNT > GCE (glassy carbon electrodes). This can be explained that a large amount of basal planes and edge planes on nanotube-modified electrodes have direct impact on theBr_2/Br^- redox reaction. Jang et al. in 2016[81] developed a type of polypropylene electrode, prepared by sheet extrusion, filled with carbon black (10 wt%), graphite (10 wt%), carbon fiber (4 wt%), maleic anhydride-grafted polypropylene (1 wt%), and carbon nanotubes (CNTs) to serve as the bipolar plate for ZBB, in which, the combination of polypropylene and CNTs give the rest of the 75 wt%. The author reported the experimental results of the electrodes with CNTs weight of 0%, 1%, 3%, 5% and 10%. They found out that the electrode with addition of 5 wt% CNTs has an optimal performance in terms of improvement of the electrical conductivity, tensile strength, and flexural module of the carbon electrodes. Wang et al.[22] in 2016 examined the electrochemical activity of Br_2/Br^- redox reaction at four commercial carbon materials: acetylene black (AB), expanded graphite (EG), carbon nanotubes (CNT) and black pearls® 2000 carbon black (BP). They used a testing cell with an effective electrode area of 9 cm^2. At a constant current density of 20 mA cm^{-2}, charging the cell for 50 minutes, and then discharging until the cell voltage is below 0.5 V, they reported that the electrochemical activity increases in the order of AB < CNT < EG < BP, in which, the activity of BP is at least double the other carbons. The high activity of BP is attributed to its large specific surface area supplying more active sites to the Br_2/Br reaction and suitable pore size distribution facilitating mass transfer.

Carbon materials with nano-sheet morphology possessing high theoretical specific surface area (2630 m^2 g^{-1})[99] and high electronic conductivity have been rarely investigated as bromine electrode. Synthesizing ordered carbon materials with the aid of metal-organic frameworks (MOFs) have been widely investigated because of their large surface area, high pore volume and tuneable structures and compositions.[20,100–103] However, the complex preparation procedures make most of the methods inefficient and expensive. Wang et al. reported a simple, economical and high yield method for formation of nano-sheet zeolite-type metal organic framework (NSZIF) via a precipitation reaction at room temperature.[20] The synthesized porous nano-sheet carbon (PNSC) showcased high specific surface area, good electronic conductivity, fast mass transport and high porosity with in-plane pores. The electrochemical activity of PNSC tested as bromine electrode in ZBB reported an energy efficiency of 82% at an operating current density of 80 mA cm^{-2}.

Ordered mesostructured carbons (OMCs) have demonstrated widespread application in batteries, fuel cells, adsorption separation and drug release, due to their high conductivity, large specific surface area and controlled morphology.[22,104–106]

The adsorption of bromine/bromine ions is the rate-determining step in the Br_2/Br^- redox reactions.[92,107] Because of their large specific surface area and bromine adsorption capacity, OMCs enhance the rate-determining step of Br_2/Br^- reactions, thereby improving the electrochemical activity.[22] Wang et al. synthesized highly stable bimodal ordered mesostructured carbons (BOMCs) by a tedious method of evaporation induced triconstituent co-assembly.[22] The BOMCs employed as cathode material in ZBB displayed good electrochemical activity owing to the 2 nm pores on the walls of 5 nm mesopores which improved specific surface area and adsorption performance, providing more active sites for bromine reactions. The highly ordered mesostructure along with oxygen-containing functional groups greatly influenced the electrochemical performance. The BOMCs tested in ZBB achieved good EE of 80.1% at an operating current density of 80 mA cm^{-2}. Wang et al. also reported a systematic study on the factors affecting the activity of different carbon materials to identify the key parameters in designing highly active carbon material for Br_2/Br^- redox reactions.[2] It was concluded that specific surface area, electrical conductivity and appropriate pore size distribution with abundant pores play a dominating role in determining the electrochemical performance of the cathode material for Br_2/Br^- redox reactions in ZBB. A highly stable and active cage-like porous carbon (CPC) with specific pore size, capable of entrapping the Br_2 complex was synthesized as a potential cathode material in ZBB.[1] The porous hollow structure was able to suppress the Br_2 crossover while maintaining good electrochemical activity owing to the high specific surface area. The ZBB assembled with CPC as the bromine electrode material reported a high CE of 98% and an EE of 81% at a current density of 80 mA cm^{-2}.

Reduced graphene oxide (rGO) is reported as a promising electro-catalytic material due to its chemical stability, good electrical conductivity and abundant surface area.[58,108–110] Suresh et al. reported rGO supported on 3D CF as bromine electrode in zinc bromine flow cell exhibiting an energy efficiency of 80.75% at an operating current density of 80 mA cm^{-2}.[58] The electrochemical analysis showed enhanced Br_2/Br^- kinetics with a reduced peak potential separation of 103 mV due to high electrochemical surface area and conductivity of rGO. As reviewed, due to their low cost, unique physical property and superior electrochemical performance, a variety of carbon materials and its derivatives have been employed as electrode materials for ZBB in the past decades. Table 2 provides some research work and result in ZBB from 1977 to 2017 to reflect the extensive effort.

4.2. In Hydrogen Bromine Redox Flow Battery

The hydrogen bromine redox flow battery (HBB) was first reported in 1980 by Yeo and Chin.[111] The electrode and cell reactions are as shown below, and the formal cell potential is 1.09 V.
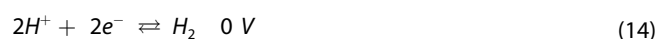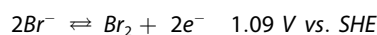
Hydrogen Negative Electrode:

$$2H^+ + 2e^- \rightleftharpoons H_2 \quad 0\ V \tag{14}$$

ChemPlusChem

Review
doi.org/10.1002/cplu.202100441

**Chemistry
Europe**
European Chemical
Societies Publishing

Table 2. Historical overview of the zinc-bromine redox flow battery.l

Year [Reference]	Operational parameters						Performance		
	Electrode materials Zn negative electrode/Bromine positive electrode	Electrolytes Negative half-cell/Positive half-cell	Membrane separator	*Cell type*	j [mA cm^{-2}]	Temp [°C]	Charge/ Discharge voltage [V]	State of Charge [%]	Efficiency [%]
1977[34]	Carbon for both electrodes (electrode area 60 cm^2)	2 M ZnBr$_2$ in 4 M KCl/ 0.05 M Br$_2$ + 2 M ZnBr$_2$ in 4 M KCl	CE-Nafion® 125	Single unit cell	20	54	1.92/1.65	NG	80 (energy)
1978[133]	Carbon powder in a plastic binder impressed upon a silver screen current collector for both electrodes (electrode area 100 cm^2)	3.0 M ZnBr$_2$, 1.0 M N-ethyl-N-methyl morpholinium bromide, 0.59 M sulpholane, 0.2 M ZnSO$_4$ 3.0 M ZnBr$_2$, 1.0 M N-ethyl-N-methyl morpholinium bromide, 0.2 M ZnSO$_4$	Microporous polyethylene CE Permion-1010	Single unit cell Eight cells connected in series	20 20	10–60 10–60	2.01/1.34 13.2 (discharge voltage)	80 74	66.7 (voltage) 82–85 (coulombic)
1985[134]	Bipolar plates consisting of carbon powder in a polypropylene binder for both electrodes (electrode area 600 cm^2)	3.0 M ZnBr$_2$, 0.5 M N-ethyl-N-methyl morpholinium bromide, 0.5 M N-ethyl-N-methyl pyrrolidinium bromide 2.0 M ZnBr$_2$, 0.5 M N-ethyl-N-methyl morpholinium bromide, 0.5 M N-ethyl-N-methyl pyrrolidinium bromide, 1 M ZnCl$_2$	microporous separator Daramic	Eight cells connected in series	20	NG	NG	67	75 (coulombic) 81–82 (coulombic)
1990[3]	Cell electrode area 1600 cm^2			Submodule 25 kW (30 cells in series, 24 stacks in parallel)	13	NG	1400/1186		65.9 (overall energy) 1300 cycles
2013[79]	Carbon polymer composite/carbon felt coated with a slurry of active carbon in ZnBr$_2$ solution	2.0 M ZnBr$_2$, 0.1 M N-ethyl-N-methyl morpholinium bromide	Daramic microporous separator	Single unit cell, single flow electrolyte	20	Room temp	1.80/1.60	NG	92 (coulombic) 89 (voltage) 82 (energy)
2013[66]	Graphite plate/carbon felt (electrode area 36 cm^2)	2.0 M ZnBr$_2$, 0.05 M N-ethyl-N-methyl pyrrolidinium bromide/2.0 M ZnBr$_2$, 0.05 M N-ethyl-N-methyl pyrrolidinium bromide	Daramic® microporous membrane coated with carbon ink	Single unit cell with two electrolyte tanks	40	25	1.93/1.60	NG	91 (coulombic) 83 (voltage) 76 (energy) 10 cycles
2016[81]	Polypropylene-carbon-carbon nanotube (5 wt%) composites for both electrodes (electrode area 36 cm^2)	2.25 M ZnBr$_2$, 0.5 M ZnCl$_2$, 0.8 M N-methyl-N-ethyl pyrrolidinium bromide	Asahi Kasei membrane SF-600	Single unit cell with two electrolyte tanks	20	25	1.90/1.50	NG	80.7 (voltage) 73.2 (energy) 1 cycle
2016[22]	Bimodal ordered mesostructure carbons for both electrodes (electrode area 9 cm^2)	2 M ZnBr$_2$, 3 M KCl/2 M ZnBr$_2$, 3 M KCl, 0.4 M N-methylethylpyrrolidinium bromide	Daramic® microporous membrane coated with carbon ink	Single unit cell with two electrolyte tanks	80	25	1.93/1.58	NG	81.8 (energy efficiency, 200 cycles)
2017[54]	Graphite felt thermally treated at 500 °C for 2 h for both electrodes (electrode area 4 cm^2)	2 M ZnBr$_2$, 4 M NH$_4$Cl	Polyacrylonitrile porous felt	Single unit cell with single flow electrolyte	40 80	23 23	1.92/1.62 2.06/1.50	NG	81.8 (energy efficiency, 50 cycles) 70 (energy efficiency, 1

Bromine Positive Electrode:

$$2Br^- \rightleftharpoons Br_2 + 2e^- \quad 1.09 \ V \ vs. \ SHE \tag{15}$$

Overall Cell Reaction:

$$2HBr \rightleftharpoons Br_2 + H_2 \quad 1.09 \ V \tag{16}$$

ChemPlusChem

Review
doi.org/10.1002/cplu.202100441

Chemistry Europe
European Chemical
Societies Publishing

At the negative electrode, hydrogen gas is evolved during charge and oxidised to protons during discharge. At the positive electrode, bromide ions are oxidised to bromine in aqueous solution during charge, and bromine is reduced to form Br_2 during discharge.[23,67,69,70]

The main advantage of the HBB is its potential for high voltaic efficiency and power density, due to the rapid kinetics of the hydrogen and bromine electrode reactions.[69,70,111] Power densities of up to 1.4 W cm^{-2} have been reported,[23,70] this being double the values reported for the vanadium RFB.[67] Coulombic efficiency is also high as a result of low self-discharge rates.[111] In addition, the hydrogen and bromine active materials are abundant and low cost,[67,112] resulting in reported system costs as low as 200 \$ kW^{-1} h^{-1}[67,113] and levelized cost of energy storage potentially as low as 0.0034 \$ kW^{-1} h^{-1}.[114]

However, there are several challenges associated with the HBB including the poisoning of platinum-based hydrogen catalysts by bromide,[70,115] high vapour pressure of bromine[70] and safety issues caused by the toxic and hazardous nature of bromine coupled with the potential for explosive reaction with hydrogen if ignited.[69] The poisoning of catalyst materials may be mitigated by encapsulating the catalyst in protective metal oxide layers or replacing platinum based catalysts with alternatives such as ruthenium sulphide doped with cobalt or nickel,[116] the latter option also having the benefit of reduced cost over platinum catalysts. The safety issues and high vapour pressure of bromine may be alleviated by the complexation of HBr to form Br^{-3}, Br^{-5} and Br^{-7},[69] or by the use of complexing agents such as polymeric salts[2,117] or quaternary ammonium bromides,[38] which lower the bromine vapour pressure.

The HBB system has received increasing attention over the past decade, Cho et al investigated the effects of flow field structure, electrolyte flow rate, bromine electrode materials and operating temperature on the performance of a HBB. By employing a high surface area bromine electrode consisting of three layers of carbon paper pre-treated in sulphuric acid to increase hydrophilicity, in conjunction with a flow through electrode configuration and an operating temperature of 55 °C, they reported a peak discharge power density of 1.4 W cm^{-2} with a high voltaic efficiency of 91% at 0.4 W cm^{-2} and the capability for high current density operation at 2.5 A cm^{-2}.[23] Their further research work has shown that, through a decrease of ion exchange membrane thickness and optimisation of electrolyte concentration, the ASR was reduced to 230 mΩ cm^{-2}, resulting in a peak discharge current density of 4 A cm^{-2} and power density of 1.46 W cm^{-2} at ambient temperature.[67]

In 2015 the same group reported on various carbon materials as bromine electrodes, including carbon paper, carbon/graphite cloths and RVC foam. However, it was found that RVC foam and graphite cloth caused high area-specific resistance (ASR) in the cell resulting in increased cell polarisation. While activated carbon cloth provided similar electrochemical performance to carbon paper, large electrolyte pressures were observed due to the lower porosity of the cloth. Carbon paper was therefore studied further and the effect of the number of layers and compression rates examined. They

report that using more than three layers of carbon paper provides no improvement in ASR, but does increase limiting current. Due to the additional cost associated with the larger number of layers, three layers of carbon paper were found to be optimal economically, as the performance gains made by additional layers did not justify the extra cost. A compression rate of ~25% was high enough to prevent flow channelling between the layers and minimise contact resistances while avoiding high electrolyte pressures caused by reduced porosity.[70] Building on previous findings, stable performance of the H_2/Br_2 flow cell was achieved over 600 charge/discharge cycles.[69]

Lin et al. reported on the use of novel electrode and membrane materials in 2015, focusing on system cost reduction.[118] Replacing the traditional Nafion membrane with an electrospun Nafion/PVDF alternative was found to reduce component cost by 60%, while utilising a nitrogen functionalised platinum-iridium hydrogen catalyst was estimated to reduce hydrogen electrode cost by 21%. This publication also introduced nanostructured bromine electrode materials to the HBB for the first time. Multi-walled carbon nanotubes (MWCNT's) were synthesised directly onto carbon paper substrates by electrodeposition of cobalt nanoparticles followed by chemical vapour deposition (CVD). A single layer of MWCNT modified carbon paper was found to outperform three layers of untreated carbon paper, resulting in a 50% decrease in bromine electrode cost. Combining these measures led to a reported stack cost of 210 \$ kW^{-1} h^{-1}, a 47% reduction compared to the baseline configuration used. Subsequent work by the same group optimised the electrodeposition/CVD process for MWCNT synthesis, reporting a dual tip/base model for MWCNT growth.[119] The optimised MWCNT modified carbon paper demonstrated an electrochemically active surface area 29 times higher than untreated carbon paper and good mechanical durability in a H_2/Br_2 flow cell.[120]

While most reports on the HBB utilise ion exchange membranes, Braff et al. have proposed a membrane free HBB configuration, resulting in cost reduction on expensive membrane materials[68,112] which could constitute around 20% of the system cost.[67] In this proposed system, the membrane is replaced by a laminar flow of HBr electrolyte between the electrodes, with a second HBr/Br_2 electrolyte utilised at the bromine electrode and a gas diffusion hydrogen electrode, as shown in Figure 4.[68,112] Fluid management is therefore a particular challenge, in order to prevent the crossover of species from the bromine electrode to the hydrogen electrode and the subsequent degradation of platinum based hydrogen catalysts.

The membrane free HBB reported by Braff et al. utilized a planar graphite bromine electrode with a flow by configuration, as shown in Figure 4a. They reported a peak power density of 0.795 W cm^{-2} with a voltaic efficiency of 91% at 200 W cm^{-2} and a maximum current density of 1.8 A cm^{-2}.[112] This was improved upon by Suss et al. who employed a single layer of carbon paper pre-treated in a 3:1 ratio of sulphuric to nitric acid at 50 °C for 5 hours to increase the hydrophilicity and activity of the electrode for the bromine reactions. The application of a porous material with increased surface area allowed for the use
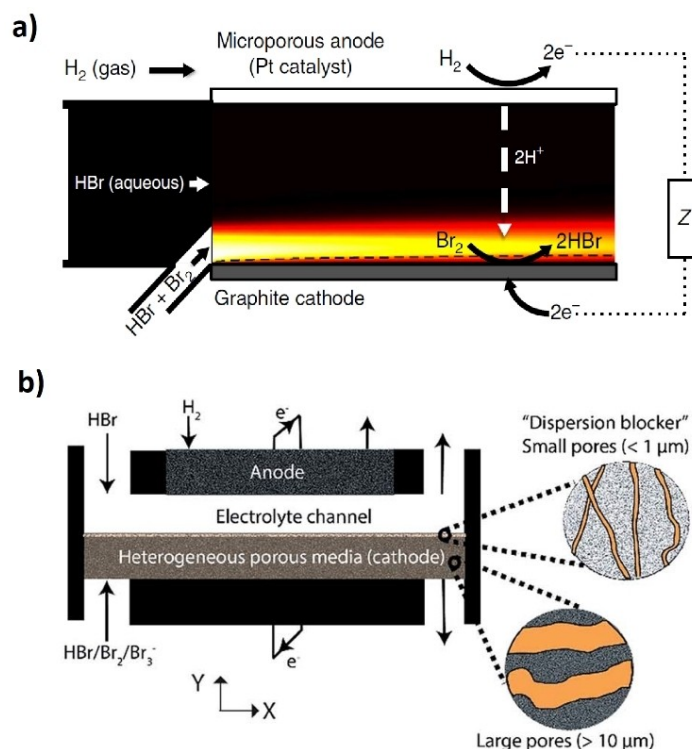
ChemPlusChem

Review

doi.org/10.1002/cplu.202100441

Chemistry
Europe
European Chemical
Societies Publishing

Figure 4. Reported configurations of membrane free H–Br flow cells; [a] Braff *et al.* 2013. Reproduced from ref. [112] with permission from Springer Nature, [b] Suss *et al.* 2016. Reproduced from ref. [68] with permission from RSC Publication.

of the flow through cell configuration shown in Figure 4b, resulting in an increased power density of 0.925 W cm^{-2} and operational current densities up to 4 A cm^{-2}.[68]

Further work on the HBB has been conducted by Zhang *et al.* and they compared the performance of graphite felt subjected to treatment in mixed sulphuric/nitric acid and thermal oxidation at temperatures between 400 and 550 °C.[66] Both methods were found to improve the hydrophilicity and activity of electrode by the introduction of oxygen containing functional groups to the carbon surface. While acid treatment at 80 °C for 8 hours was more effective than thermal oxidation at introducing oxygen containing functional groups, they report that thermal oxidation at 500 °C produced the best performing graphite felt electrode materials, with lower charge transfer resistance resulting in improved power density in an H$_2$/Br$_2$ fuel cell. This was attributed to superabundant oxidation following acid treatment causing increased ohmic resistances, in conjunction with increased electrochemically active surface areas following thermal oxidation resulting from cavities formed by the oxidation of carbon monoxide to carbon dioxide, as shown in Figure 5. More recently, Karaeyvaz *et al.* have reported on the use of novel hollow core mesoporous shell (HCMS) as a cathode material for the HBB.[121] This was prepared using a template replication method using solid core mesoporous silica as a template, with the resultant HCMS carbon consisting of particles around 200 nm in diameter, with high surface areas of up to 1832 m^{2}g^{-1}. A hydrogen bromine cell employing HCMS achieved power densities over 30 % higher than with commercial carbon black.

In summary, with fast and highly reversible reaction kinetics of both the hydrogen and bromine electrodes, and with low cost and abundance of both active material, the HBB is able to achieve high power density and high efficiency. Further R&D work is still required to reduce cost and optimise performance, including careful cell design to reduce ASR and ohmic losses and development high surface area carbon-based electrode materials to improve bromine reactions.

4.3. In Polysulphide Bromine Redox Flow Battery

Polysulphide-Bromine flow battery (PSBB) systems were introduced by Remick and Ang in 1984[122] and had developed by Regenesys® Technologies (UK) from 1991 to 2004.[123–125] This system is based on the Br$_2$/Br$^-$ redox couple at positive electrode and S$_4^{2-}$/S$_2^{2-}$ couple at negative electrode and employs NaBr electrolyte in the positive half-cell and Na$_2$S$_4$ electrolyte in the negative half-cell, respectively. These chemicals of electrolytes are abundant in the nature and easily available at very low cost, which provides PSBB an advantage of being more economical for scaling-up of energy storage capacity among RFB family. The electrode and cell reactions are:
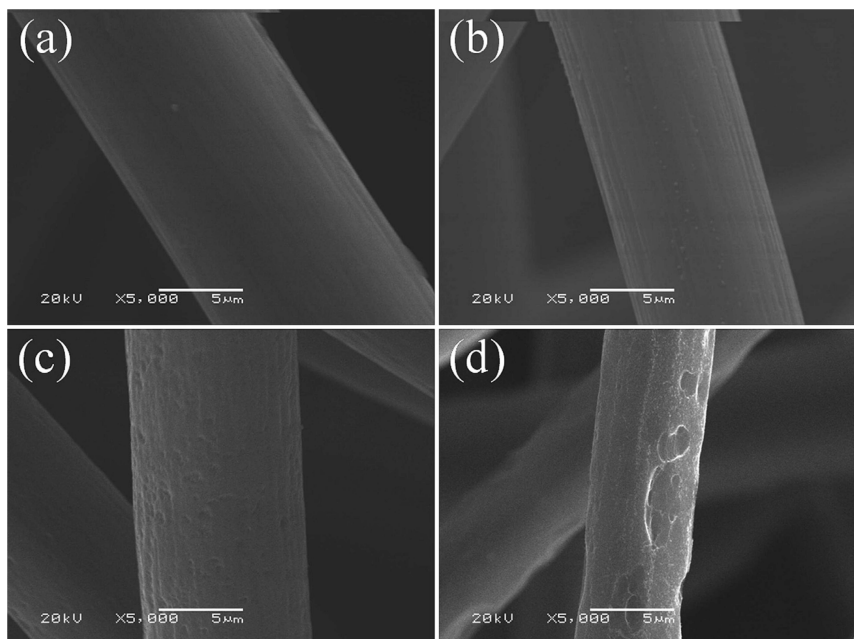
negative electrode

$$S_4^{2-} + 2e^- \rightleftharpoons 2S_2^{2-} \tag{17}$$

Figure 5. SEM images of the graphite felt electrodes before and after thermal oxidation: [a] as received, [b] 400 °C for 5 h, [c] 500 °C for 5 h and [d] 550 °C for 5 h. Reproduced from ref. [66] with permission from Elsevier.
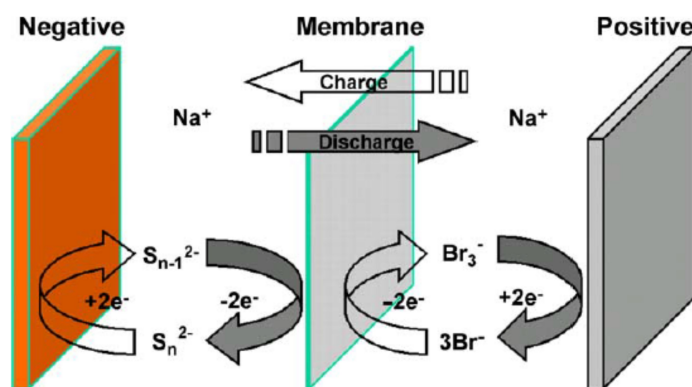

Figure 6. Schematic of a polysulphide/bromine redox flow battery. Reproduced from ref. [53] with permission from Elsevier.

positive electrode

$$3Br^- - 2e^- \rightleftharpoons Br_3^- \qquad (18)$$

cell reaction

$$S_4^{2-} + 3Br^- \rightleftharpoons 2S_2^{2-} + Br_3^- \qquad (19)$$

The standard cell voltage is 1.515 V. However, depending on activity of the active species and the state of charge or discharge, a PSBB can give a wider range of 1.54–1.60 V open-circuit cell voltage.[126] As illustrated in Figure 6, during charge, at the positive electrode Br^- ions are oxidized to Br_2 and complexed as Br_3^- ions while the soluble polysulphide S_4^{2-} anions are reduced to sulphide S_2^{2-} ions at the negative electrode. During discharge, the reverse reaction occurs. The sulphide ions are oxidised to polysulphide S_4^{2-} anions at anode

while the tribromide ions are reduced to bromide ions at cathode. A cation exchange membrane is used to separator between the positive half-cell and negative half-cell in order to prevent the sulphur anions reacting directly with bromine. The electrical balance is achieved by the transport of Na^+ ions across the membrane.[5,126] Unlike other bromine-based RFB systems, it is usually no bromine sequestration agents required in the PSBB system.

The early work in the 1980s carried out by the PSBB inventors of Remick and Ang[122] examined reticulated vitreous carbon and transition metal dichalcogenides as positive electrodes for bromine/bromide reaction and transition metal sulphides as negative electrodes for sulphide/polysulphide redox reaction. For example, they utilized a flow-by solid graphite plate as positive electrode and a flow-through porous sulphided sintered nickel as negative electrode with an electrode area of 35 cm² and Nafion 125 membrane as the separator. The open-

ChemPlusChem

Review

doi.org/10.1002/cplu.202100441

Chemistry Europe
European Chemical
Societies Publishing

circuit cell voltage was reported to be 1.74 V at full charge state and 1.50 V at 50% state-of-charge when operated at 25 °C in 1 M NaBr saturated with bromine in positive half-cell and 2 M Na_2S_4 in negative half-cell.

The research work carried out from 1990 mainly utilized carbon-based material for bromine electrode including carbon felt, graphite felt, carbon cloth, and carbon paper, which are highly abundant and easily available. For example, between 1991 and 2004, by using laser-based production engineering techniques, Regenesys® Technologies used carbon-polyolefin composite electrodes which enable the electrodes to be welded to the polyolefin cell frames, scaled up the PSBB system at three sizes with nominal power ratings of the stacks 5 kW, 20 kW, and 100 kW, respectively. A 1 MW pilot scale facility was installed and tested with a round-trip efficiency of 60–65% and energy density of 20–30 Wh L.[5,125,127–130]

Zhang et al.[53,126,131,132] examined various bromine electrode materials including PAN-based carbon felt, graphite felt and activated carbon. When graphite felt was used as the positive electrode and the cobalt-coated graphite felt as the negative electrode, the cell achieved stable coulombic efficiency of 96.1%, voltage efficiency of 84.3%, and energy efficiency of 81% over 50 cycles (600 h) at a current density of 40 mA cm^{-2}. In addition, they reported that the activated carbon was prepared from coconut shells mixed with PVDF powder, carbon black of Vulcan XC-72, and NaBr in a weight ratio of 15:3:2:2. The mixture was then moulded and compressed at a temperature of 200 °C and a pressure of 4 MPa to obtain activated carbon with a high surface area of 1366 m^{2}g^{-1} which is more than 30,000 times that of the graphite felt and carbon felt. However, the authors discovered that the high surface area of the activated carbon electrode didn't add to the cell cycling performance because they observed some element sulphur crystals were deposited on the external surface of used activated carbon electrode. This sulphur deposit blocked the pores and decreased mass transport of active species, and thus led to the deterioration of the performance of the activated carbon electrode.

5. Summary and Outlook

As reviewed, the highly tuneable nature of carbon materials results in great promise for their development as bromine electrode materials. Various carbon materials such as carbon felts, papers, cloths and other their derives have been widely investigated and the benefits of surface activation by the introduction of oxygen containing functional groups by thermal or acid treatment methods to increase hydrophilicity is well established. Therefore, significant advances of carbon based bromine electrodes that are capable ofproviding large surface area materials with high catalytic activity for bromine reactions would facilitate the development of highly efficient, cost effective bromine based flow battery systems.

Stability and durability tests are necessary for those carbon-based bromine electrodes. By reviewing the existing literature, it is perhaps not surprising that the reported results are usually based on small lab-cells and that often the long-term cycle performance is not established. It is important, for a practical application, that the performance of the cell is monitored under durability and lifetime test (e.g. long-term cycle test over extended periods, tests under unbalancing the discharge and charge rates, asymmetric cycling and intermittent stop-start tests) to reveal the effect of a dynamic load on the stability of the cell and to mimic realistic in-service operation.

Literature on degradation studies of these carbon based materials appeared sparse. It would contribute to a better understanding if more research is conducted to characterize the material on a molecular level in order to determine the degree of order in graphite layers, the type of defects, state of additives etc. Complementary surface science probes such as FTIR and Raman spectroscopy can be employed in concert with weight loss and chemical analysis of used electrolytes to characterise the surface functional degradation of carbon by oxidation, bromination, erosion and corrosion.

In short, good carbon based bromine electrode material should have high electrocatalytic activity and high surface area, and be robust and capable of low-cost and volume production. With advancements in technology, such materials will be expected to display superior performance than the current state of the art of technology, thereby facilitating efficient and durable bromine based flow batteries.

Acknowledgements

Conflict of Interest

The authors declare no conflict of interest.

[1] C. Wang, Q. Lai, P. Xu, D. Zheng, X. Li, H. Zhang, *Adv. Mater.* **2017**, *29*, 1605815.

[2] C. Wang, X. Li, X. Xi, P. Xu, Q. Lai, H. Zhang, *RSC Adv.* **2016**, *6*, 40169.

[3] P. C. Butler, P. A. Eidler, P. G. Grimes, S. E. Klassen, R. C. Miles in *Handbook of batteries* (Eds.: D. Linden T. B. Reddy), McGraw-Hill, New York, **2002**, pp. 39.1–22.

[4] Z. Yang, J. Zhang, M. C. W. Kintner-Meyer, X. Lu, D. Choi, J. P. Lemmon, J. Liu, *Chem. Rev.* **2011**, *111*, 3577.

[5] P. Leung, X. Li, C. Ponce de León, L. Berlouis, C. T. J. Low, F. C. Walsh, *RSC Adv.* **2012**, *2*, 10125.

[6] L. F. Arenas, A. Loh, D. P. Trudgeon, X. Li, C. Ponce de León, F. C. Walsh, *Renewable Sustainable Energy Rev.* **2018**, *90*, 992.

[7] C. Zhang, L. Zhang, Y. Ding, S. Peng, X. Guo, Y. Zhao, G. He, G. Yu, *Energy Storage Mater.* **2018**, *15*, 324.

[8] M. L. Perry, A. Z. Weber, *J. Electrochem. Soc.* **2015**, *163*, A5064.

[9] P. Alotto, M. Guarnieri, F. Moro, *Renewable Sustainable Energy Rev.* **2014**, *29*, 325.

[10] A. Z. Weber, M. M. Mench, J. P. Meyers, P. N. Ross, J. T. Gostick, Q. Liu, *J. Appl. Electrochem.* **2011**, *41*, 1137.

[11] J. Noack, N. Roznyatovskaya, T. Herr, P. Fischer, *Angew. Chem. Int. Ed.* **2015**, *54*, 9776.

[12] V. Viswanathan, A. Crawford, D. Stephenson, S. Kim, W. Wang, B. Li, G. Coffey, E. Thomsen, G. Graff, P. Balducci, M. Kintner-Meyer, V. Sprenkle, *J. Power Sources* **2014**, *247*, 1040.

[13] M. Rychcik, M. Skyllas-Kazacos, *J. Power Sources* **1988**, *22*, 59.

[14] W. Wang, Q. Luo, B. Li, X. Wei, L. Li, Z. Yang, *Adv. Funct. Mater.* **2013**, *23*, 970.

[15] R. Feng, X. Zhang, V. Murugesan, A. Hollas, Y. Cheng, Y. Shao, E. Walter, N. P. N. Wellala, L. Yan, W. Wang, *Science* **2021**, *372*, 836.

[16] J. Huang, S. Hu, X. Yuan, Z. Xiang, M. Huang, K. Wan, J. Piao, Z. Fu, Z. Liang, *Angew. Chem. Int. Ed.* **2021**, *60*, 20921.

[17] S. Hu, T. Li, M. Huang, J. Huang, W. Li, L. Wang, Z. Chen, Z. Fu, X. Li, Z. Liang, *Adv. Mater.* **2021**, *33*, 2005839

[18] S. Hu, L. Wang, X. Yuan, Z. Xiang, M. Huang, P. Luo, Y. Liu, Z. Fu, Z. Liang, *Energy Mater. Adv.* **2021**, *2021*, 9795237.

[19] X. Li, P. Gao, Y.-Y. Lai, J. D. Bazak, A. Hollas, H.-Y. Lin, V. Murugesan, S. Zhang, C.-F. Cheng, W.-Y. Tung, Y.-T. Lai, R. Feng, J. Wang, C.-L. Wang, W. Wang, Y. Zhu, *Nat. Energy* **2021**, *6*, 873.

[20] C. Wang, Q. Lai, K. Feng, P. Xu, X. Li, H. Zhang, *Nano Energy* **2018**, *44*, 240.

[21] I. Rubinstein, *J. Phys. Chem.* **1981**, *85*, 1899.

[22] C. Wang, X. Li, X. Xi, W. Zhou, Q. Lai, H. Zhang, *Nano Energy* **2016**, *21*, 217.

[23] K. T. Cho, P. Ridgway, A. Z. Weber, S. Haussener, V. Battaglia, V. Srinivasan, *J. Electrochem. Soc.* **2012**, *159*, A1806.

[24] Y. Lv, Y. Li, C. Han, J. Chen, Z. He, J. Zhu, L. Dai, W. Meng, L. Wang, *J. Colloid Interface Sci.* **2020**, *566*, 434.

[25] G. Wei, C. Jia, J. Liu, C. Yan, *J. Power Sources* **2012**, *220*, 185.

[26] P. C. K. Vesborg, T. F. Jaramillo, *RSC Adv.* **2012**, *2*, 7933.

[27] J. Llopis, M. Vàzquez, *Electrochim. Acta* **1962**, *6*, 167.

[28] J. Llopis, M. Vasquez, *Electrochim. Acta* **1962**, *6*.

[29] G. Faita, G. Fiori, T. Mussini, *Electrochim. Acta* **1968**, *13*, 1765.

[30] W. D. Cooper, R. Parsons, *Trans. Faraday Soc.* **1970**, *66*.

[31] R. E. White, S. E. Lorimer, *J. Electrochem. Soc.* **1983**, *130*, 1096.

[32] L. J. J. Janssen, J. G. Hoogland, *Electrochim. Acta* **1970**, *15*, 1677.

[33] M. Mastragostino, C. Gramellini, *Electrochim. Acta* **1985**, *30*, 373.

[34] H. S. Lim, A. M. Lackner, R. C. Knechtli, *J. Electrochem. Soc.* **1977**, *124*, 1154.

[35] D. J. Eustace, *J. Electrochem. Soc.* **1980**, *127*, 528.

[36] K. J. Cathro, K. Cedzynska, D. C. Constable, *J. Power Sources* **1985**, *16*, 53.

[37] K. J. Cathro, K. Cedzynska, D. C. Constable, P. M. Hoobin, *J. Power Sources* **1986**, *18*, 349.

[38] K. Cedzynska, *Electrochim. Acta* **1995**, *40*, 971.

[39] G. Bauer, J. Drobits, C. Fabjan, H. Mikosch, P. Schuster, *J. Electroanal. Chem.* **1997**, *427*, 123.

[40] W. Kautek, A. Conradi, C. Fabjan, G. Bauer, *Electrochim. Acta* **2001**, *47*, 815.

[41] I. Vogel, A. Mobius, *Electrochim. Acta* **1991**, *36*, 1403.

[42] T. X. Huong Le, M. Bechelany, M. Cretin, *Carbon* **2017**, *122*, 564.

[43] S. Whitley, D. Bae, *J. Electrochem. Soc.* **2021**, *168*, 120517.

[44] M. Wang, J. Du, J. Zhou, C. Ma, L. Bao, X. Li, X. Li, *J. Power Sources* **2019**, *424*, 27.

[45] X. Zhou, T. Zhao, Y. Zeng, L. An, L. Wei, *J. Power Sources* **2016**, *329*, 247.

[46] J. M. Friedrich, C. Ponce-de-León, G. W. Reade, F. C. Walsh, *J. Electroanal. Chem.* **2004**, *561*, 203.

[47] L. Zhang, S. Zhao, *Chem. Soc. Rev.* **2009**, *38*, 2520.

[48] M. H. Chakrabarti, N. P. Brandon, S. A. Hajimolana, F. Tariq, V. Yufit, M. A. Hashim, M. A. Hussain, C. T. J. Low, P. V. Aravind, *J. Power Sources* **2014**, *253*, 150.

[49] M. Wu, T. Zhao, R. Zhang, L. Wei, H. Jiang, *Electrochim. Acta* **2018**, *284*, 569.

[50] X. Zhou, Y. Zeng, X. Zhu, L. Wei, T. Zhao, *J. Power Sources* **2016**, *325*, 329.

[51] SGL Carbon, https://www.sglcarbon.com/en/markets-solutions/material/sigracell-battery-felts/; file:///C:/Users/xl327/Downloads/SGL-Datasheet-SIGRACELL-Battery-Felts-EN%20(2).pdf.

[52] PAN carbon felt, https://www.fuelcellstore.com/fuel-cell-components/gas-diffusion-layers/carbon-felt/avcarb-c100-soft-carbon-felt.

[53] H. Zhou, H. Zhang, P. Zhao, B. Yi, *Electrochim. Acta* **2006**, *51*, 6304.

[54] M. Wu, T. Zhao, H. Jiang, Y. Zeng, Y. Ren, *J. Power Sources* **2017**, *355*, 62.

[55] SGL Carbon GFA5, https://www.sglcarbon.com/en/markets-solutions/material/sigratherm-soft-felt/; file:///C:/Users/xl327/Downloads/SGL-Datasheet-SIGRATHERM-GFA-EN%20(1).pdf.

[56] R. P. Naresh, K. Mariyappan, K. S. Archana, S. Suresh, D. Ditty, M. Ulaganathan, P. Ragupathy, *ChemElectroChem* **2019**, *6*, 5688.

[57] F. Jiang, Z. He, D. Guo, X. Zhou, *J. Power Sources* **2019**, *440*, 227114.

[58] S. Suresh, M. Ulaganathan, R. Pitchai, *J. Power Sources* **2019**, *438*, 226998.

[59] PCP Fuel cell store, https://www.fuelcellstore.com/fuel-cell-components/gas-diffusion-layers/carbon-paper/cetech-carbon-paper/ct-gdl280-carbon-pape.

[60] C. Sun, F. M. Delnick, L. Baggetto, G. M. Veith, T. A. Zawodzinski, *J. Power Sources* **2014**, *248*, 560.

[61] SGL carbon paper, https://www.fuelcellstore.com/fuel-cell-components/gas-diffusion-layers/carbon-paper/sigracet?page=1.

[62] K. V. Greco, A. Forner-Cuenca, A. Mularczyk, J. Eller, F. R. Brushett, *ACS Appl. Mater. Interfaces* **2018**, *10*, 44430.

[63] Y. A. Hugo, W. Kout, F. Sikkema, Z. Borneman, K. Nijmeijer, *J. Energy Storage* **2020**, *27*, 101068.

[64] SpectraCarb 2050 A Fuel cell store, https://www.fuelcellstore.com/fuel-cell-components/gas-diffusion-layers/carbon-paper/spectracarb/spectracarb-2050a–1550.

[65] Carbon cloth Fuel Cell store, https://www.fuelcellstore.com/fuel-cell-components/gas-diffusion-layers/carbon-cloth/elat/hydrophilic-cloth.

[66] L. Zhang, Z. Shao, X. Wang, H. Yu, S. Liu, B. Yi, *J. Power Sources* **2013**, *242*, 15.

[67] K. T. Cho, P. Albertus, V. Battaglia, A. Kojic, V. Srinivasan, A. Z. Weber, *Energy Technol.* **2013**, *1*, 596.

[68] M. E. Suss, K. Conforti, L. Gilson, C. R. Buie, M. Z. Bazant, *RSC Adv.* **2016**, *6*, 100209.

[69] K. T. Cho, M. C. Tucker, M. Ding, P. Ridgway, V. S. Battaglia, V. Srinivasan, A. Z. Weber, *ChemPlusChem* **2015**, *80*, 402.

[70] M. C. Tucker, K. T. Cho, A. Z. Weber, G. Lin, T. Van Nguyen, *J. Appl. Electrochem.* **2015**, *45*, 11.

[71] M. E. Lee, H. J. Jin, Y. S. Yun, *RSC Adv.* **2017**, *7*, 43227.

[72] T. X. H. Le, R. Esmilaire, M. Drobek, M. Bechelany, C. Vallicari, S. Cerneaux, A. Julbe, M. Cretin, *J. Phys. Chem. C* **2017**, *121*, 15188.

[73] Y. S. Park, B. Y. Hong, S. J. Cho, J. H. Boo, *Bull. Korean Chem. Soc.* **2011**, *32*.

[74] D. Bae, G. Kanellos, G. M. Faasse, E. Draževic, A. Venugopal, W. A. Smith, *Commun. Mater.* **2020**, *1*, 17

[75] P. C. Ghimire, R. Schweiss, G. G. Scherer, T. M. Lim, N. Wai, A. Bhattarai, Q. Yan, *Carbon* **2019**, *155*, 176.

[76] R. Schweiss, C. Meiser, F. W. T. Goh, *ChemElectroChem* **2017**, *4*, 1969.

[77] T. J. Rabbow, M. Trampert, P. Pokorny, P. Binder, A. H. Whitehead, *Electrochim. Acta* **2015**, *173*, 17.

[78] Z. Xu, Q. Fan, Y. Li, J. Wang, P. D. Lund, *Renewable Sustainable Energy Rev.* **2020**, *127*, 109838.

[79] Q. Lai, H. Zhang, X. Li, L. Zhang, Y. Cheng, *J. Power Sources* **2013**, *235*, 1.

[80] S. Suresh, M. Ulaganathan, N. Venkatesan, P. Periasamy, P. Ragupathy, *J. Energy Storage* **2018**, *20*, 134.

[81] W. I. Jang, J. W. Lee, Y. M. Baek, O. O. Park, *Macromol. Res.* **2016**, *24*, 276.

[82] X. Sun, T. Souier, M. Chiesa, A. Vassallo, *Electrochim. Acta* **2014**, *148*, 104.

[83] C. M. Hagg, J. O. Besenhard, M. S. Kazacos, Fourteenth Annual Battery Conference on Applications and Advances. Proceedings of the Conference (Cat. No.99TH8371), 349–354.

[84] K. J. Cathro, K. Cedzynska, D. C. Constable, *J. Power Sources* **1987**, *19*, 337.

[85] G. Long, X. Li, K. Wan, Z. Liang, J. Piao, P. Tsiakaras, *Appl. Catal. B* **2017**, *203*, 541.

[86] K. Wan, A. Tan, Z. Yu, Z. Liang, J. Piao, P. Tsiakaras, *Appl. Catal. B* **2017**, *209*, 447.

[87] C. Jin, H. Lei, M. Liu, A. Tan, J. Piao, Z. Fu, Z. Liang, H. Wang, *Chem. Eng. J.* **2020**, *380*, 122606.

[88] L. Wu, Y. Shen, L. Yu, J. Xi, X. Qiu, *Nano Energy* **2016**, *28*, 19.

[89] L. Shi, S. Liu, Z. He, J. Shen, *Electrochim. Acta* **2014**, *138*, 93.

[90] T. Wu, K. Huang, S. Liu, S. Zhuang, D. Fang, S. Li, D. Lu, A. Su, *J. Solid State Electrochem.* **2012**, *16*, 579.

ChemPlusChem

Review

doi.org/10.1002/cplu.202100441

Chemistry Europe
European Chemical
Societies Publishing

[91] M. Liu, Z. Xiang, J. Piao, J. Shi, Z. Liang, *Electrochim. Acta* **2018**, *259*, 687.

[92] M. Wu, H. Jiang, R. Zhang, L. Wei, K. Chan, T. Zhao, *Electrochim. Acta* **2019**, *318*, 69.

[93] H. Xiang, A. Tan, J. Piao, Z. Fu, Z. Liang, *Small* **2019**, *15*, 1901848.

[94] S. Agnoli, M. Favaro, *J. Mater. Chem. A* **2016**, *4*, 5002.

[95] V. Thirumal, A. Pandurangan, R. Jayavel, R. Ilangovan, *Synth. Met.* **2016**, *220*, 524.

[96] X. Yu, P. Han, Z. Wei, L. Huang, Z. Gu, S. Peng, J. Ma, G. Zheng, *Joule* **2018**, *2*, 1610.

[97] N. Venkatesan, K. S. Archana, S. Suresh, R. Aswathy, M. Ulaganthan, P. Periasamy, P. Ragupathy, *ChemElectroChem* **2019**, *6*, 1107.

[98] Y. Munaiah, S. Suresh, S. Dheenadayalan, V. K. Pillai, P. Ragupathy, *J. Phys. Chem. C* **2014**, *118*, 14795.

[99] S. Yang, X. Feng, L. Wang, K. Tang, J. Maier, K. Müllen, *Angew. Chem. Int. Ed.* **2010**, *49*, 4795.

[100] K. Shen, X. Chen, J. Chen, Y. Li, *ACS Catal.* **2016**, *6*, 5887.

[101] W. Ren, H. Zhang, C. Guan, C. Cheng, *Adv. Funct. Mater.* **2017**, *27*, 1702116.

[102] C. Guan, X. Liu, W. Ren, X. Li, C. Cheng, J. Wang, *Adv. Energy Mater.* **2017**, *7*, 1602391.

[103] C. Guan, W. Zhao, Y. Hu, Z. Lai, X. Li, S. Sun, H. Zhang, A. K. Cheetham, J. Wang, *Nanoscale Horiz.* **2017**, *2*, 99.

[104] Y. Shao, X. Wang, M. Engelhard, C. Wang, S. Dai, J. Liu, Z. Yang, Y. Lin, *J. Power Sources* **2010**, *195*, 4375.

[105] A. Vinu, M. Miyahara, T. Mori, K. Ariga, *J. Porous Mater.* **2006**, *13*, 379.

[106] G. S. Chai, I. S. Shin, J.-S. Yu, *Adv. Mater.* **2004**, *16*, 2057.

[107] J. D. Jeon, H. S. Yang, J. Shim, H. S. Kim, J. H. Yang, *Electrochim. Acta* **2014**, *127*, 397.

[108] K. H. Thebo, X. Qian, Q. Zhang, L. Chen, H.-M. Cheng, W. Ren, *Nat. Commun.* **2018**, *9*, 1486.

[109] J. Zhong, W. Sun, Q. Wei, X. Qian, H. Cheng, W. Ren, *Nat. Commun.* **2018**, *9*, 1.

[110] H. Wang, Y. Hu, *Energy Environ. Sci.* **2012**, *5*, 8182.

[111] R. S. Yeo, D. T. Chin, *J. Electrochem. Soc.* **1980**, *127*, 549.

[112] W. A. Braff, M. Z. Bazant, C. R. Buie, *Nat. Commun.* **2013**, *4*, 2346.

[113] N. Singh, E. W. McFarland, *J. Power Sources* **2015**, *288*, 187.

[114] Y. A. Hugo, W. Kout, G. Dalessi, A. Forner-Cuenca, Z. Borneman, K. Nijmeijer, *Techno-Economic Analysis of a Kilo-Watt Scale Hydrogen-Bromine Flow Battery System for Sustainable Energy Storage* **2020**.

[115] M. Goor-Dar, N. Travitsky, E. Peled, *J. Power Sources* **2012**, *197*, 111.

[116] A. Ivanovskaya, N. Singh, R. F. Liu, H. Kreutzer, J. Baltrusaitis, T. Van Nguyen, H. Metiu, E. McFarland, *Langmuir* **2013**, *29*, 480.

[117] M. Mastragostino, S. Valcher, *Electrochim. Acta* **1983**, *28*, 501.

[118] G. Lin, P. Y. Chong, V. Yarlagadda, T. V. Nguyen, R. J. Wycisk, P. N. Pintauro, M. Bates, S. Mukerjee, M. C. Tucker, A. Z. Weber, *J. Electrochem. Soc.* **2015**, *163*, A5049.

[119] V. Yarlagadda, G. Lin, P. Y. Chong, T. Van Nguyen, *J. Electrochem. Soc.* **2016**, *163*, A5126.

[120] V. Yarlagadda, G. Lin, P. Y. Chong, T. Van Nguyen, *J. Electrochem. Soc.* **2015**, *163*, A5134.

[121] M. C. Karaeyvaz, B. Duman, B. Fıçıcılar, *Int. J. Hydrogen Energy* **2021**, *46*, 29512.

[122] R. J. Remick, P. G. P. Ang, US 4485154, **1984**.

[123] R. Zito, US 5612148, **1997**.

[124] G. Cooley, *Power Eng.* **1999**, *13*, 122.

[125] F. C. Walsh, *Pure Appl. Chem.* **2001**, *73*, 1819.

[126] H. Zhang, in *Advances in batteries for large- and medium-scale energy storage: Applications in power systems and electric vehicles* (Eds.: C. Menictas, M. Skyllas-Kazacos, T. M. Lim), Woodhead Publishing, **2015**, pp. 317–327.

[127] T. J. Calver, S. E. Male, P. J. Mitchell, I. Whyte, WO 99/57775, **1999**.

[128] P. Morrissey, P. J. Mitchell, S. E. Male, WO 0103221, **2001**.

[129] P. Morrissey, N. Ward, GB 2374722B, **2002**.

[130] Regenesys utility scale energy storage project summary, DTI report, **2004**.

[131] S. Ge, B. Y. Yi, H. Zhang, *J. Appl. Electrochem.* **2004**, *34*, 181.

[132] P. Zhao, H. Zhang, H. Zhou, B. Yi, *Electrochim. Acta* **2005**, *51*, 1091.

[133] A. F. Venero, US 4105829, **1978**.

[134] E. Kantner, US 4491625 A, **1985**.